Broad receptor engagement of an emerging global coronavirus may potentiate its diverse cross-species transmissibility

Wentao Li[a,1], Ruben J. G. Hulswit[a,1], Scott P. Kenney[b,1], Ivy Widjaja[a], Kwonil Jung[b], Moyasar A. Alhamo[b], Brenda van Dieren[a], Frank J. M. van Kuppeveld[a], Linda J. Saif[b,2], and Berend-Jan Bosch[a,2]

[a]Virology Division, Department of Infectious Diseases & Immunology, Faculty of Veterinary Medicine, Utrecht University, 3584 CL Utrecht, The Netherlands; and [b]Department of Veterinary Preventive Medicine, Food Animal Health Research Program, Ohio Agricultural Research and Development Center, The Ohio State University, Wooster, OH 44691

Contributed by Linda J. Saif, April 12, 2018 (sent for review February 15, 2018; reviewed by Tom Gallagher and Stefan Pöhlmann)

Porcine deltacoronavirus (PDCoV), identified in 2012, is a common enteropathogen of swine with worldwide distribution. The source and evolutionary history of this virus is, however, unknown. PDCoV belongs to the *Deltacoronavirus* genus that comprises predominantly avian CoV. Phylogenetic analysis suggests that PDCoV originated relatively recently from a host-switching event between birds and mammals. Insight into receptor engagement by PDCoV may shed light into such an exceptional phenomenon. Here we report that PDCoV employs host aminopeptidase N (APN) as an entry receptor and interacts with APN via domain B of its spike (S) protein. Infection of porcine cells with PDCoV was drastically reduced by APN knockout and rescued after reconstitution of APN expression. In addition, we observed that PDCoV efficiently infects cells of unusual broad species range, including human and chicken. Accordingly, PDCoV S was found to target the phylogenetically conserved catalytic domain of APN. Moreover, transient expression of porcine, feline, human, and chicken APN renders cells susceptible to PDCoV infection. Binding of PDCoV to an interspecies conserved site on APN may facilitate direct transmission of PDCoV to nonreservoir species, including humans, potentially reflecting the mechanism that enabled a virus, ancestral to PDCoV, to breach the species barrier between birds and mammals. The APN cell surface protein is also used by several members of the *Alphacoronavirus* genus. Hence, our data constitute the second identification of CoVs from different genera that use the same receptor, implying that CoV receptor selection is subjected to specific restrictions that are still poorly understood.

PDCoV | spike | APN | receptor | cross-species transmission

Coronaviruses (CoVs) are enveloped positive-strand RNA viruses—classified into four genera: *Alpha*-, *Beta*-, *Gamma*-, and *Deltacoronavirus* (subfamily *Coronavirinae*, family *Coronaviridae*)—that exhibit a propensity for interspecies transmission (1, 2). The betacoronaviruses severe acute respiratory syndrome (SARS)-CoV and Middle East respiratory syndrome (MERS)-CoV, both of which can cause lethal respiratory infections in humans, are notable examples of CoVs crossing species barriers. SARS-CoV became human-adapted after a zoonotic introduction in 2002 and quickly spread to infect thousands worldwide before its containment in 2003 (3, 4). MERS-CoV, discovered a decade later, has not adapted to sustained replication in humans as yet, but causes recurrent spillover infections from its reservoir host, the dromedary camel (5). Phylogenetic studies indicate that cross-species transmission has occurred rather frequently during CoV evolution and shaped the diversification of CoVs (6). In fact, the endemic human coronaviruses HCoV-HKU1, HCoV-229E, HCoV-NL63, and HCoV-OC43 all have a zoonotic origin (7–11). Occurrence of such cross-species transmission events may be attributed to widespread CoV prevalence in mammals and birds, and to their extraordinary variability stemming from high mutation rates and high frequency recombination, which greatly increase the potential for successful adaptation to a new host (6, 12). A pivotal criterion of cross-species transmission concerns the ability of a virus to engage a receptor within the novel host, which for CoVs, is determined by the receptor specificity of the viral spike (S) entry protein.

The porcine deltacoronavirus (PDCoV) is a recently discovered CoV of unknown origin. PDCoV (species name coronavirus HKU15) was identified in Hong Kong in pigs in the late 2000s (13) and has since been detected in swine populations in various countries worldwide (14–24). It infects the intestinal epithelia and can cause acute, watery diarrhea and vomiting, resulting in dehydration and body weight loss with potentially fatal consequences (23, 25, 26). So far, all other members of the *Deltacoronavirus* genus have been detected in birds, suggesting that birds are the natural host and ancestral reservoir of deltacoronaviruses (13). PDCoV is most closely related to the sparrow CoV HKU17. Pairwise genome analysis shows that these two viruses are subspecies of the same species with >96% amino acid identity in domains used for species demarcation (13, 27), indicating that an interspecies transmission event from birds to

Significance

Coronaviruses exhibit a propensity for interspecies transmission, with SARS- and MERS-coronaviruses as notable examples. Cross-species transmission by coronaviruses is foremost determined by the virus' ability to bind receptors of new hosts. We here report that the recently identified, yet globally distributed porcine deltacoronavirus employs host aminopeptidase N (APN) as an entry receptor via S protein-mediated interaction with an interspecies conserved domain that allows for APN orthologue-mediated entry. Identification of APN as a deltacoronavirus receptor emphasizes the remarkable preferential employment of cell surface host peptidases as receptors by coronaviruses. Our findings provide important insight into how receptor usage of coronaviruses may fuel cross-host transmission between distantly related species and necessitate surveillance studies of deltacoronaviruses in thus far unappreciated potential reservoirs, including humans.

Author contributions: W.L., R.J.G.H., S.P.K., I.W., L.J.S., and B.-J.B. designed research; W.L., R.J.G.H., S.P.K., I.W., K.J., M.A.A., and B.v.D. performed research; L.J.S. contributed new reagents/analytic tools; W.L., R.J.G.H., S.P.K., I.W., K.J., M.A.A., F.J.M.v.K., L.J.S., and B.-J.B. analyzed data; and R.J.G.H. and B.-J.B. wrote the paper.

Reviewers: T.G., Loyola University Chicago; and S.P., German Primate Center.

The authors declare no conflict of interest.

[1]W.L., R.J.G.H., and S.P.K. contributed equally to this work.

[2]To whom correspondence may be addressed. Email: saif.2@osu.edu or b.j.bosch@uu.nl.

This article contains supporting information online at www.pnas.org/lookup/suppl/doi:10.1073/pnas.1802879115/-/DCSupplemental.

Published online May 14, 2018.

MICROBIOLOGY

mammals may have occurred relatively recently. Interestingly, the S proteins of the bulbul CoV HKU11 and munia CoV HKU13 show higher sequence identity with the PDCoV S protein compared with that of HKU17 (70.2% and 71.2% vs. 44.8%), suggesting that a recombination event preluded emergence of this porcine CoV (13).

Studying PDCoV spike–receptor interactions may provide insight into the presumed host-switching event from birds to swine. The CoV S protein forms homotrimers and is composed of an N-terminal S1 subunit and a C-terminal S2 subunit, responsible for receptor binding and membrane fusion, respectively. Recent cryo-EM reconstructions of the CoV trimeric S structures of alpha-, beta-, and deltacoronaviruses (28–32) revealed that the S1 subunit comprises four core domains ($S1^{A–D}$), of which domains A and B have been implicated in receptor binding. So far, a surprisingly limited set of four cell surface host glycoproteins have been reported to be used as receptors by CoVs. The carcinoembryonic antigen-related cell-adhesion molecule 1 is recognized as a receptor by the lineage A betacoronavirus MHV (33). The three remaining receptors are all membrane ectopeptidases, one of which is used by members from different genera. The aminopeptidase N (APN) is targeted by a number of alphacoronaviruses, including HCoV-229E and transmissible gastroenteritis virus (TGEV) (34, 35). Dipeptidyl peptidase 4 (DPP4) was shown to be used as a receptor by the lineage C betacoronavirus MERS-CoV (36). Finally, the peptidase angiotensin converting enzymes 2 (ACE2) is used as a receptor by the alphacoronavirus HCoV-NL63, as well as by the (lineage B) betacoronavirus SARS-CoV (37, 38). In addition to proteinaceous host molecules, (acetylated) sialic acid carbohydrates may be used as primary receptors or as attachment factors (39–42). The entry receptor for PDCoV is unknown, as well as for any of the other deltacoronaviruses identified thus far. In this study, we aimed to identify and characterize the receptor usage of this globally distributed pathogen, which may provide important insight into the virus' evolutionary trajectory, interspecies transmissibility, and pathogenesis.

Results

The S1 Receptor Binding Subunit of the PDCoV S Protein Interacts with Host APN. In our search for PDCoV host receptor determinants, we screened known CoV receptors and detected binding of the S1 subunit of PDCoV S to porcine APN (pAPN). pAPN is a 963 amino acid-long type-II transmembrane glycoprotein, expressed as a homo-dimer on the cell surface. Transient expression of C-terminal HA-tagged pAPN in HeLa cells rendered these cells receptive to binding with Fc-tagged PDCoV S1 protein (Fig. 1*A* and *SI Appendix*, Fig. S1), similar to the S1 protein of TGEV that served as a positive control. Cell surface staining to pAPN-expressing cells was also observed with the isolated domain B of PDCoV S1 ($S1^{B}$), indicating that this spike domain is responsible for pAPN binding (31, 32). HCoV-229E S1—known to bind human APN (hAPN) but not the porcine ortholog—did not bind to pAPN-expressing cells (43). Solid-phase binding experiments confirmed the interaction between the PDCoV S1 and $S1^{B}$ with the pAPN ectodomain (Fig. 1*B*); albeit TGEV S1 bound pAPN more efficiently, indicative of a higher binding affinity. These data demonstrate that the S1 receptor binding subunit of the PDCoV S protein directly interacts with the host APN transmembrane ectopeptidase with the interacting site residing in S1 domain B.

pAPN Is a Functional Entry Receptor for PDCoV. PDCoV can replicate in swine testis (ST) cells with supplemental trypsin (23). To determine the role of pAPN interaction in PDCoV entry, we used a mutant ST cell line lacking cell surface APN expression (ST-$pAPN^{KO}$) that had been made previously using CRISPR/Cas9 genome editing (44). In addition, we generated an ST-$pAPN^{KO}$ cell line with reconstituted pAPN expression (ST-$pAPN^{KO}$-pAPN). Integrity of the mutant cell lines was confirmed by sequencing, TGEV S1 cell surface staining (44) (*SI Appendix*, Fig. S2*A*), Western blotting (*SI Appendix*, Fig. S2*B*), and infection with TGEV control virus (Fig. 2*A*). Parental ST cells, ST-$pAPN^{KO}$, and ST-$pAPN^{KO}$-pAPN cells were inoculated with PDCoV at a multiplicity of infection (MOI) of 1 in the presence of trypsin and the percentage of infected cells was assessed after immunostaining. As revealed by flow cytometric and immune-fluorescence quantification, APN ablation in ST

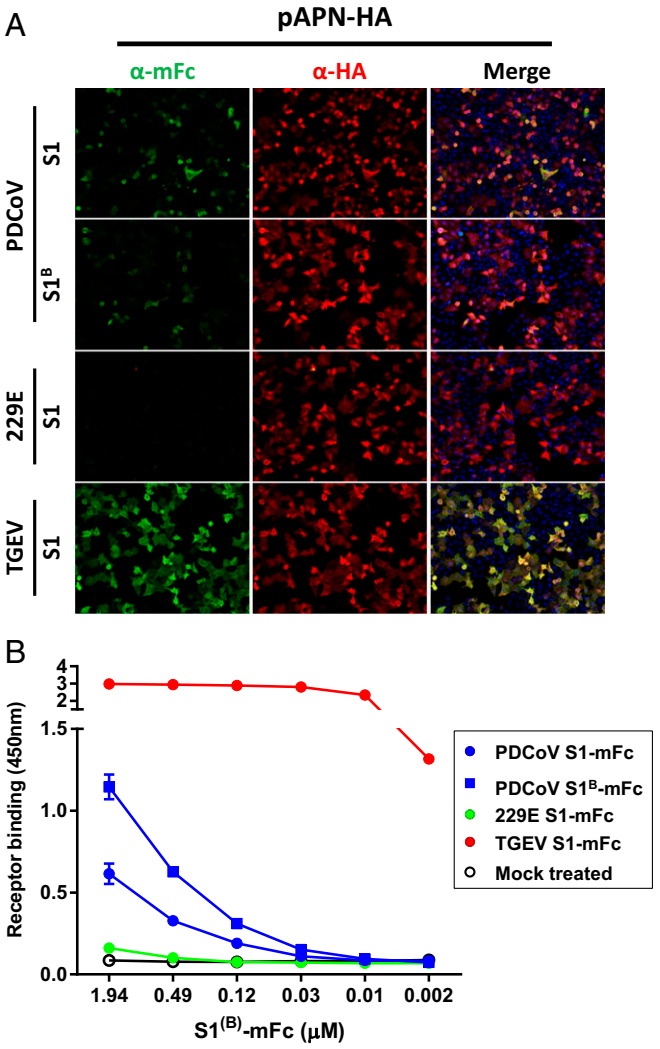

Fig. 1. The S1 and the $S1^{B}$ domain of the PDCoV S protein bind to pAPN. (*A*) PDCoV S1 and $S1^{B}$ domain bind to HeLa cells overexpressing pAPN. HeLa cells mock-transfected or transfected with a plasmid encoding HA-tagged pAPN were incubated with equimolar amounts of PDCoV S1 or $S1^{B}$ proteins that were C-terminally tagged with the Fc domain of murine IgG2a (S1-mFc and $S1^{B}$-mFc). Binding of the mFc-tagged S1 proteins and APN expression was measured by immunofluorescence assay using antibodies recognizing the mFc-tag or HA-tag, respectively. S1-mFc fusion proteins of the S proteins of TGEV (interacts with pAPN) and HCoV-229E (does not interact with pAPN) were taken along as controls. (Magnification: 200×.) (*B*) PDCoV S1 and $S1^{B}$ bind soluble pAPN. The 96-well plates coated with pAPN ectodomain were incubated with serially diluted PDCoV S1-mFc and $S1^{B}$-mFc proteins. Bound $S1^{(B)}$-mFc proteins were detected via HRP-conjugated antibodies recognizing the mFc-tag and subsequent development using HRP substrate. TGEV and HCoV-229E S1-mFc proteins were used as a positive and negative APN binding control, respectively. Error bars = SD; $n = 2$ (independent experiments each with two technical replicates).

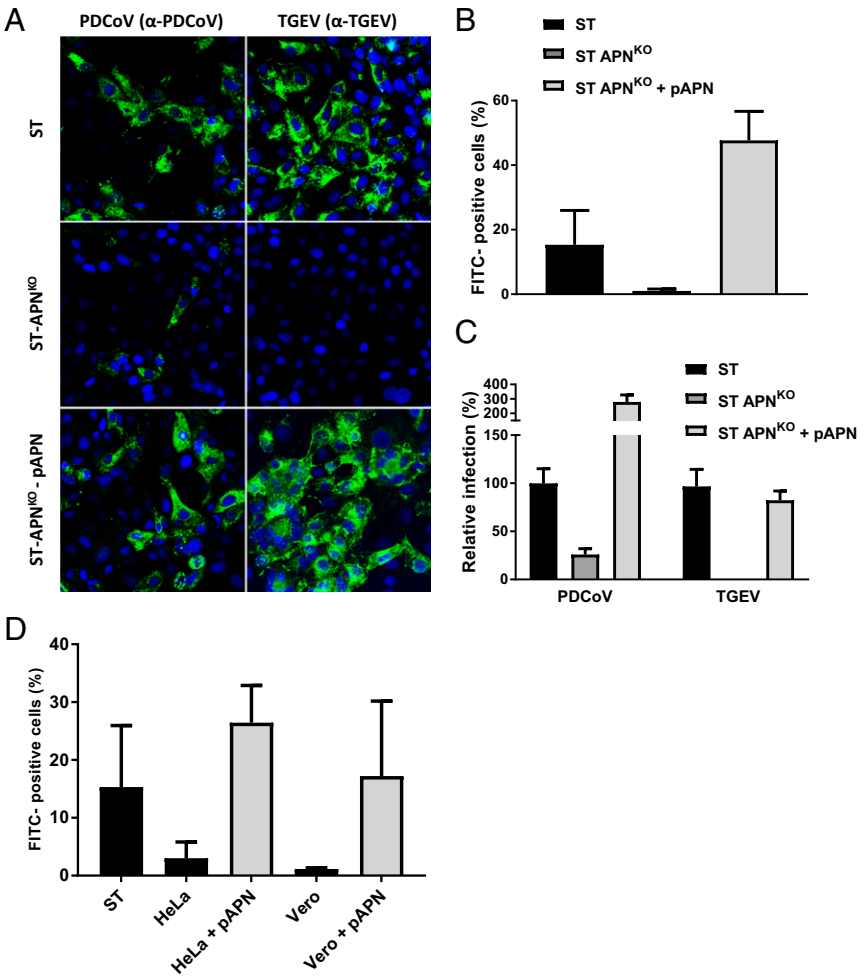

Fig. 2. Impact of APN expression on PDCoV infection. (*A*) PDCoV employs APN during ST cell entry. ST, ST-APN^{KO}, and pAPN reconstituted knockout cells were inoculated with PDCoV or TGEV at a MOI of 1. Cells were fixed and permeabilized 16 hpi and stained using a PDCoV-specific antiserum or a TGEV-specific monoclonal antibody, respectively. Infection experiments were performed twice; representative pictures are shown. (Magnification: 300×.) (*B*) PDCoV infection levels on pAPN deficient and reconstituted ST cells were quantified by flow cytometry. Infection levels are shown normalized to parental ST cell infection. Experiments were repeated four times; averages are shown. (*C*) PDCoV and TGEV infection levels on pAPN-deficient and reconstituted ST cells quantified by counting virus-infected cells after immunofluorescent staining. Infection levels are shown relative to infection on the parental ST cells. Infection experiments were performed twice; a representative experiment is shown. (*D*) APN overexpression in HeLa and Vero cells potentiates PDCoV infection. HeLa and Vero cells stably expressing pAPN were generated by retroviral transduction. Cells were inoculated with PDCoV at a MOI = 1 (as titrated on ST cells) and infection levels were quantified at 16 hpi by flow cytometry. Experiments were performed two to five times. Average infection levels are shown relative to infection on the ST cells.

cells reduced PDCoV infection by ∼75–90% relative to parental ST cells, whereas pAPN reconstitution in ST-APN^{KO} cells enhanced PDCoV infection beyond levels observed on parental ST cells, indicating that PDCoV uses pAPN as a receptor for infection (Fig. 2 *B* and *C*).

During infection, expression of CoV S glycoprotein at the plasma membrane can result in formation of multinucleated syncytia, which depends on and positively correlates with the local cell-surface receptor concentration. Following PDCoV infection, efficient syncytium formation was observed in ST and Vero cells overexpressing pAPN (ST-pAPN^{KO}-pAPN and Vero-pAPN) but not in parental cells (*SI Appendix*, Fig. S3) [and, as earlier reported in wild-type ST cells (23)] that express low levels of APN (*SI Appendix*, Fig. S2*A*), suggesting that the APN glycoprotein can be employed by PDCoV S to mediate cell–cell fusion.

To further verify the role of pAPN in PDCoV infection, we used human HeLa and African green monkey Vero cells that were poorly susceptible to PDCoV infection, correlating with a lack of detectable APN expression in these cells (45–47). Mutant HeLa and Vero cell lines stably expressing pAPN were generated, and parental and mutant cell lines, as well as ST cells, were inoculated with PDCoV. pAPN expression rendered HeLa and Vero cells susceptible to PDCoV infection at levels similar to those observed on ST cells (Fig. 2*D*). In addition, we determined whether infection of parental and APN^{KO} ST cells as well as Vero cells stably expressing pAPN and its parental counterpart would support viral replication. To this end, we assessed the PDCoV growth kinetics through a multistep growth-curve experiment on these cell lines, supernatants of which were taken at set times and titrated on LLC-PK1 cells (*SI Appendix*, Fig. S4). The results indicate that the presence of APN enhances production of infectious PDCoV particles (∼100× increase in viral titers) and suggests that these cell lines are indeed permissive to productive PDCoV infection. Collectively, our data indicate that pAPN can act as an entry receptor for PDCoV infection.

PDCoV Can Infect Cells of Galline and Human Origin. The presumed origin of PDCoV in birds (13) and the well-known cross-species transmission potential of CoVs (6) led us to investigate the

susceptibility of cell lines from species other than swine to PDCoV infection. To this end, we performed PDCoV infection experiments (MOI = 1.0) on cell lines derived from human and galline tissues. Remarkably, galline hepatoma (Leghorn male hepatoma, LMH) and fibroblast (DF-1) cells, as well as human hepatoma (Huh7) cells, appeared susceptible to PDCoV infection (Fig. 3). To determine whether APN contributes to PDCoV infection of Huh7 cells, we used an APN-deficient Huh7 cell line (Huh7-APN^{KO}) that was made previously by CRISPR/Cas9 genome editing (44). The integrity of the mutant cell line was confirmed by Western blotting (*SI Appendix*, Fig. S2*B*), sequencing, and infection with HCoV-229E control virus. Knockout of APN in Huh7 cells greatly reduced infection with PDCoV (Fig. 3), indicating that PDCoV requires hAPN for efficient infection of Huh7 cells.

Because we had observed a lack of complete APN-dependency of PDCoV in both porcine and human cells in the context of genetic APN knockout, we opted to determine whether APN expression levels of wild-type cell lines correlated with PDCoV susceptibility. To this end, we inoculated several porcine (LLC-PK1, PKFA, ST, ST APN^{KO}, SK6, PD5, and PK-15) and human (Huh7, Huh7 APN^{KO}, HeLa, and HRT-18) cell lines with PDCoV or APN-dependent control viruses (TGEV or HCoV-229E) at a MOI = 2.0 for 1 h and assessed infection levels by immunostaining. In parallel, APN cell surface expression levels of these cell lines were quantified by flow cytometric staining with TGEV (porcine cells) or HCoV-229E (human cells) S1-Fc proteins (*SI Appendix*, Fig. S5). APN expression levels appeared to be consistently higher in cell lines that displayed enhanced susceptibility to PDCoV, whereas absence of detectable APN cell surface expression was associated with limited PDCoV infection levels.

PDCoV S Interacts with Galline and Human APN. We then examined whether the PDCoV S protein can bind cell surface-expressed hAPN and galline APN (gAPN). Again, HeLa cells were transfected with plasmids encoding either hAPN or gAPN, and subjected to CoV S1 cell surface staining. S1 proteins of TGEV and HCoV-229E were used for comparison. No TGEV S1 binding was seen to cells expressing hAPN or gAPN, whereas HCoV-229E S1 binding was observed only to hAPN-expressing cells. Clear binding of PDCoV S1 as well as of S1^{B} was seen to cells expressing hAPN or gAPN (Fig. 4*A*), consistent with the susceptibility of human and galline cells to PDCoV infection.

Subsequently, we performed a solid-phase binding experiment to validate the observed recognition of human and galline APN by the PDCoV S protein via domain S1^{B}. Binding of mFc-tagged PDCoV S1^{B} was tested in 96-well plates coated with ectodomains of hAPN and gAPN, as well as of pAPN (positive control). TGEV and HCoV-229E S1 control proteins specifically interacted with porcine and human APN, respectively, whereas no binding by either of the two proteins was observed to gAPN. PDCoV S1^{B} displayed clear binding to hAPN and gAPN (Fig. 4*B*), in addition to the porcine equivalent. Binding of human and particularly gAPN by PDCoV S1^{B} was higher relative to pAPN, suggesting differences in affinity.

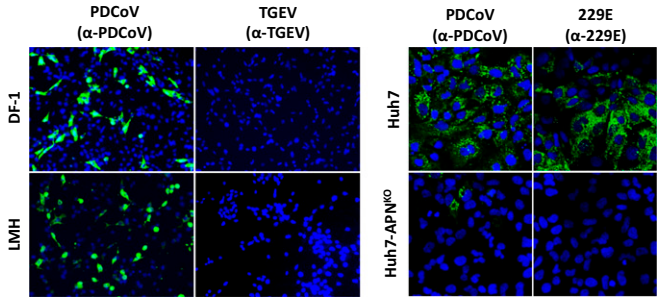

Fig. 3. PDCoV infect cells of human and avian origin. Cell lines of avian (LMH and DF-1) and human (Huh7, Huh7-APN^{KO}) origin were inoculated with PDCoV, TGEV, or HCoV-229E (MOI = 1) for 1 h, after which infection was assessed by immunostaining at 16 hpi. The results were confirmed in an independent experiment; pictures of a representative experiment are shown. (Magnification: *Left*, 200×; *Right*, 300×.)

PDCoV S1^{B} Interacts with the Catalytic Domain of APN. Structural analyses of the APN ectodomain has revealed four independently folded domains, termed domains I through IV (48), which are highly conserved across animal species of the different vertebrate classes (Fig. 5*A* and *SI Appendix*, Fig. S6). Two of these domains are known to be targeted by the S1 subunits of other CoV species: HCoV-229E S1 engages APN via domain II, whereas TGEV S1 binds to domain IV (34, 49). To assess whether one of these two domains is also targeted by PDCoV, we designed a flow-cytometric binding assay using interspecies APN chimeras. Human and feline APN (fAPN) were selected for chimera construction, as the wild-type proteins were observed to be bound strongly and undetectably by PDCoV S1^{B}, respectively, under flow-cytometric assay conditions, while these APN orthologs were also compatible with the use of S1 proteins of HCoV-229E (binds hAPN, no detectable binding to fAPN) and TGEV (can bind fAPN, no detectable binding to hAPN) as binding controls. Hence, we exchanged APN domains II or IV in hAPN by the corresponding fAPN domains and vice versa, and assessed the PDCoV S1^{B} binding patterns to cell-surface wild-type and chimeric APN by flow-cytometry, alongside with TGEV and HCoV-229E S1 control proteins. Cell surface expression of the constructed APN chimeras was confirmed via staining by control CoV S1 proteins (Fig. 5*B*) or via detection of the C-terminally added HA-tag (*SI Appendix*, Fig. S7). Whereas PDCoV S1^{B} binding to hAPN was lost upon exchange of domain II for the feline equivalent, PDCoV binding to hAPN was maintained when domain IV was swapped (Fig. 5*B*). Correspondingly, fAPN recognition by PDCoV S1^{B} remained below the detection level after exchange with human domain IV, but was significantly increased upon swapping of domain II (Fig. 5*B*). Taken together, our data indicate that, like HCoV-229E, PDCoV engagement of APN critically depends on the catalytic domain II. However, it should be noted that, because fAPN is bound to low affinity by PDCoV S1 and can be used as an entry receptor by the virus (*vide infra*), no results can be drawn from any negative results obtained in this assay.

PDCoV Can Use APN of Mammalian and Avian Species for Cell Entry. Finally, we assessed whether the mammalian and avian APN orthologs that were observed to interact with PDCoV S1 can serve as an entry receptor for this virus in vitro. We also included fAPN because analysis by solid-phase binding assay showed that PDCoV recognizes this APN ortholog, albeit to a low level (*SI Appendix*, Fig. S8) that remained undetectable in our flow cytometric analysis, shown in Fig. 5*B*. Hence, HeLa cells transfected with plasmids encoding APN orthologs were inoculated with PDCoV, HCoV-229E, or TGEV (MOI = 1). Percentage of infected cells was determined via immunostaining and counting. As reported previously (34, 50), expression of human or feline APN rendered cells susceptible to HCoV-229E infection, while expression of porcine or feline APN enabled infection with TGEV (35, 50). No infection with HCoV-229E or TGEV was seen in cells transfected with gAPN. In contrast, expression of the porcine, feline, human, and galline APN orthologs were all found to greatly enhance PDCoV infection on HeLa cells (Fig. 6), compared with mock-transfected cells. In summary, these data indicate that PDCoV can use an exceptional range of mammalian as well as avian APN molecules as an entry receptor in vitro.

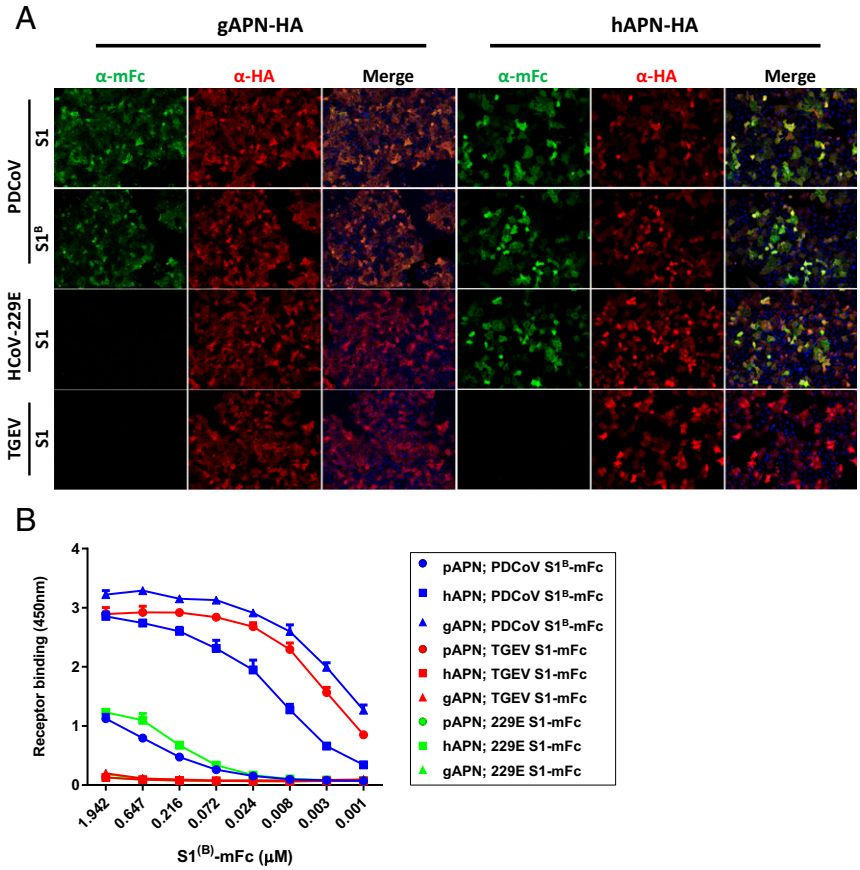

Fig. 4. PDCoV S1 binds to APN of human and avian origin. (*A*) PDCoV S1- and $S1^B$ bind to HeLa cells overexpressing galline and human APN. HeLa cells transiently transfected with a plasmid encoding HA-tagged human or gAPN (hAPN-HA and gAPN-HA) were incubated with equimolar amounts of Fc-tagged PDCoV S1 and $S1^B$ fusion proteins. Binding of the S1 proteins and APN expression was measured by immunofluorescence assay using antibodies recognizing the Fc-tag or HA-tag, respectively. Fc-tagged S1 proteins of the spike proteins of TGEV (binds pAPN) and HCoV-229E (does not bind pAPN) were used as controls. (Magnification: 200×.) (*B*) PDCoV S1 and $S1^B$ interact with human and galline APN. MaxiSorp-well plates coated with the ectodomain of porcine, human, or galline APN were incubated with serial dilutions of PDCoV S1-mFc and $S1^B$-mFc proteins. Bound $S1^{(B)}$-mFc proteins were detected via HRP-conjugated antibodies recognizing the mFc-tag and subsequent development using HRP substrate. TGEV and HCoV-229E S1-mFc proteins were used as a positive and negative APN binding control, respectively. Error bars = SD; $n = 2$ (independent experiments each with two technical replicates).

Discussion

Receptor interaction is the first, essential step in virus infection of the host cell, and hence the key factor in defining a host range of viruses. We here demonstrate that PDCoV employs domain B of its S1 subunit to engage host APN as a receptor for cell entry. APN expression confers susceptibility of cells to infection by this pathogen. Infection with PDCoV was drastically reduced after knockout of APN in porcine or human cells, although no full block in infection was observed, indicating that APN-independent entry routes can be used by the virus in cell culture and permitting the possibility that PDCoV infection requires a coreceptor. The unusual receptor promiscuity of PDCoV and the ability of PDCoV to infect cells of avian and mammalian species warrant further investigation into the virus' epidemiology and cross-species transmissibility.

APN is a multifunctional protein displaying enzymatic and other functions, including peptide processing, cholesterol uptake and chemotaxis to cell signaling, and cell adhesion (51). APN is widely distributed and highly conserved in amino acid sequence across species of the Animalia kingdom (*SI Appendix*, Fig. S6) and is expressed in a wide range of tissues, including the epithelial cells of kidneys (51), respiratory tract (52, 53), and gastrointestinal tract (54). Despite the wide distribution of APN in various tissues, PDCoV infection appears to be restricted to the swine enteric tract (55), indicating that factors other than receptor distribution play a role in CoV tissue tropism, such as differential distribution of cellular spike-activating proteases, which have been shown to play a decisive role in the CoV entry process (56). Remarkably, PDCoV shares its APN receptor with several members of the *Alphacoronavirus* genus, including TGEV and HCoV-229E (34, 35, 50), and thereby constitutes the second example of a CoV receptor that is shared across CoV genera, in addition to ACE2, which is recognized by the S proteins of alphacoronavirus HCoV-NL63 and betacoronavirus SARS-CoV (37, 38). While TGEV and other viruses of the *Alphacoronavirus-1* species bind APN via domain IV (49, 57), the alphacoronavirus HCoV-229E (58) and deltacoronavirus PDCoV engage domain II of their receptor. Despite involvement of the same receptor domain, the (proposed) receptor binding loops emanating from the $S1^B$ domains of the PDCoV and HCoV-229E S proteins lack sequence homology (*SI Appendix*, Fig. S9), similar to what has been observed for the receptor binding domains of SARS-CoV and HCoV-NL63 (59) and indicative of independent receptor acquisition during evolution. These observations suggest that APN has been independently selected as a receptor on at least two and likely three occasions during CoV evolution. The notable preferential employment of APN as a receptor by CoVs remains enigmatic but may stem from the abundant expression of this surface glycoprotein on epithelial cells of the intestinal (54) and respiratory tracts (52, 53), its inherent accessibility as a

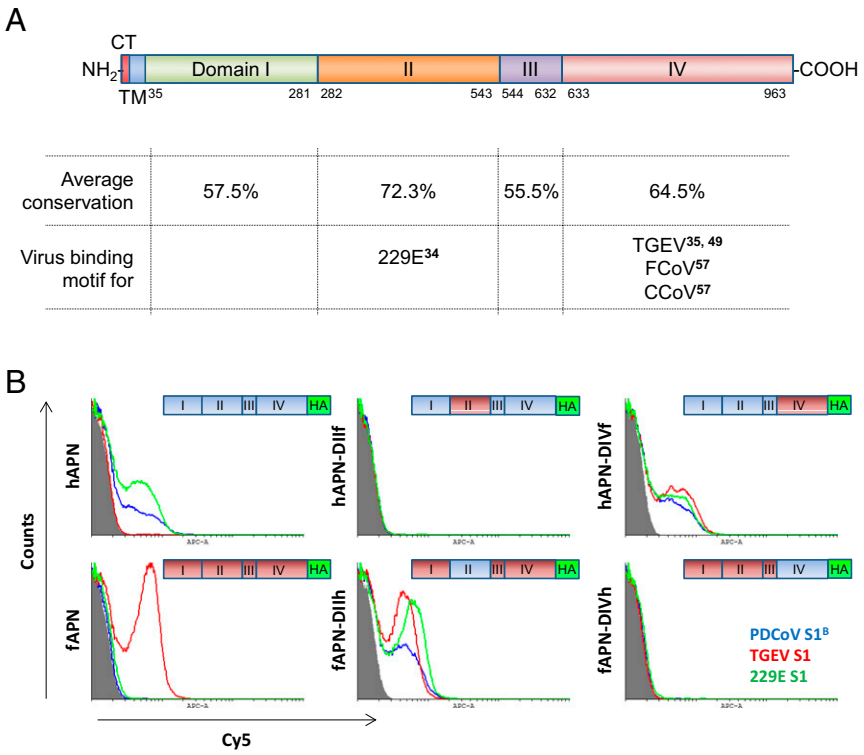

Fig. 5. The highly conserved domain II of APN is engaged by PDCoV S domain $S1^B$. (*A*) Schematic representation of the APN protein with the different domains and virus binding regions indicated. Schematic is based on the 963-amino acid sequence of pAPN (GenBank accession no. NP_999442.1) and was designed in accordance with the pAPN crystal structure as determined by Santiago et al. (75) (PDB ID code 5LDS). CT, cytosolic tail; TM, transmembrane domain. Virus binding regions of HCoV-229E, TGEV, feline coronavirus (FCoV), and canine coronavirus (CCoV) are indicated, as previously reported (34, 35, 49, 57). APN conservation across different classes of the subphylum *Vertebrata* was determined using APN amino acid sequences from mammals, amphibians, reptiles, birds, and fish. A complete alignment of the APN amino acid sequences used is shown in *SI Appendix*, Fig. S4. (*B*) PDCoV $S1^B$ interacts with the catalytic domain of APN (domain II). APN^- HeLa cells were transfected with plasmids encoding human, feline or chimeric APN proteins, and were examined the next day for interaction with PDCoV $S1^B$, HCoV-229E S1, and TGEV S1-mFc fusion proteins by FACS analysis using a donkey α-mouse Cy5 conjugate (1:200). To control for cell surface expression, samples were stained with a rabbit α-HA antibody and corresponding conjugate (see *SI Appendix*, Fig. S7). $S1^{(B)}$-mFc protein binding to cells is color-coded (PDCoV $S1^B$, red; HCoV-229E, green; TGEV, blue) and compared with the HCoV-NL63 S1-mFc (negative control). Schematic representations of the C-terminally HA-tagged APN chimeras used in the assay are indicated in the plots. Data were analyzed using Cyflogic software.

peptidase, and the reported clustering of APN in specific (plasma)membrane microdomains with host cell transmembrane proteases that proteolytically prime CoV S proteins for membrane fusion (60). Considering the extensive CoV diversity in bats and their proposed role as the ultimate ancestral reservoir (61, 62), we posit that the proteinaceous receptor usage of CoVs is likely not limited to the four known cell surface glycoproteins and that the repeated identification of these receptor molecules is merely a reflection of (effective) cross-species transmission compatibility with hosts of veterinary and medical importance.

Successful cross-species transmission depends foremost on the virus' ability to bind and functionally use a receptor within an alternative host, causing the S protein to be the driver of CoV emergence. However, (changes in) non-S genes may codetermine virus emergence in novel hosts (63). Our data indicate that PDCoV has access to cells of an exceptionally diverse range of species by binding to an interspecies conserved domain on APN. This resembles the situation for MERS-CoV, which recognizes its entry receptor DPP4 via a conserved binding site facilitating recurring zoonotic infections from its dromedary reservoir without the need for host receptor adaptation (64, 65). Selection of phylogenetically conserved receptors may provide viruses an evolutionary advantage by giving them leeway to explore alternative hosts, occasionally resulting in host switching and virus speciation (66). Considering its presumed avian origin, PDCoV's functional engagement of orthologous receptors offers an attractive explanation for a mechanism that enabled a virus, ancestral to PDCoV, to breach the species barrier between birds and mammals. Structural studies on the PDCoV $S1^B$–APN complex may reveal the molecular basis for PDCoV's remarkable receptor usage.

Our observations collectively reveal the multihost potential of PDCoV. A broad host range of PDCoV is also suggested by the reported susceptibility of germ-free calves to experimental PDCoV infection (67), as well as by the identification of a highly similar virus—at the time not yet recognized as a deltacoronavirus—in Chinese ferret badgers and Asian leopard cats at live-animal markets in southern China (68). As opposed to the repeated identification and isolation of PDCoV from swine, the incidental identification of viruses in both cat and badger with identical sequences seem to argue against a role for these animals as a potential reservoir (13). Whether these examples therefore represent spillover events from the pig reservoir, or have arisen from a yet unidentified (avian) host, remains to be seen.

The global distribution in swine of PDCoV with multihost potential is alarming from an epidemiological point of view. Pigs are the second largest livestock species (69) and acted as intermediate hosts for zoonotic viruses (70, 71), emphasizing the need for studying the zoonotic potential of the PDCoV and its surveillance in so far unappreciated potential reservoirs, including humans.

Materials and Methods

Antibodies, Cells, and Viruses. Polyclonal rabbit serum detecting HCoV-229E was kindly provided by Pierre J. Talbot, INRS-Institut Armand-Frappier,

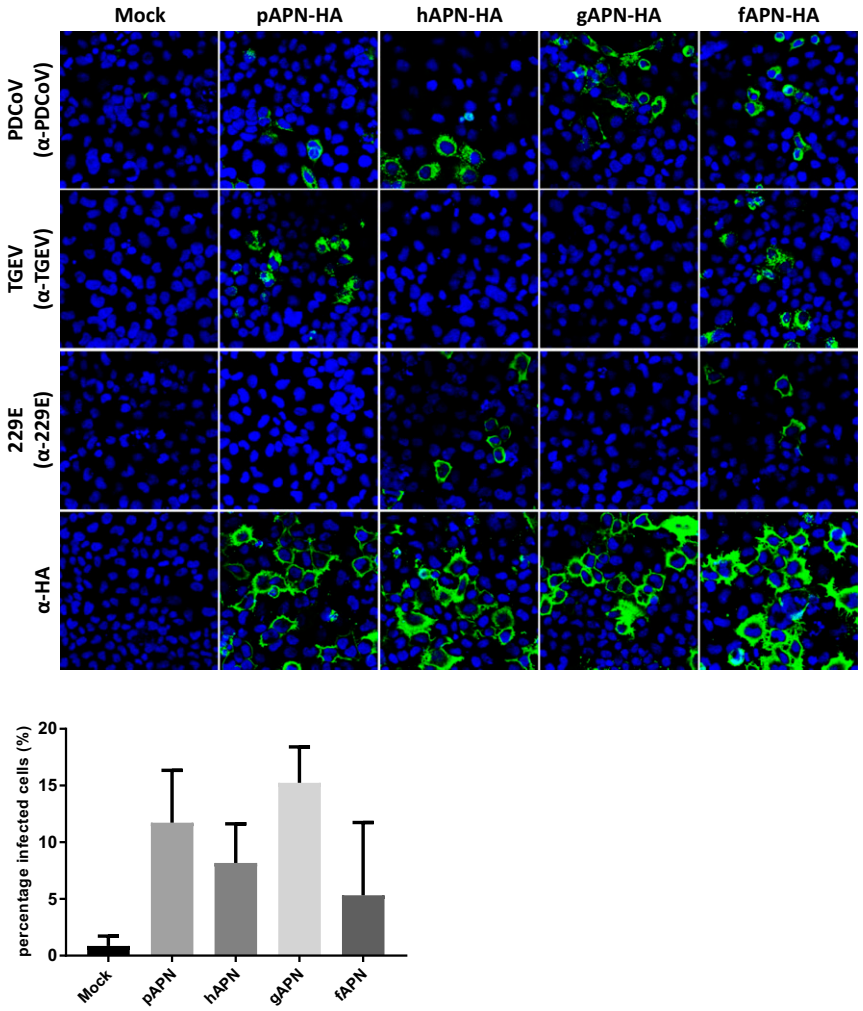

Fig. 6. PDCoV can use APN orthologs of nonhost species as a receptor. Orthologous APN molecules facilitate PDCoV entry into cells. (*Upper*) HeLa cells mock-transfected or transfected with plasmids encoding pAPN, hAPN, gAPN, and fAPN, were inoculated with PDCoV, HCoV-229E, or TGEV at a MOI = 1 for 1 h. Cells were fixed and permeabilized 24 hpi and stained with virus specific antibodies (PDCoV, TGEV, and HCoV-229E) or a mouse anti-HA antibody (Abcam, ab130275) and corresponding Alexa594 conjugate. Infection experiments were performed twice; pictures of a representative experiment are shown. (Magnification: 300×.) (*Lower*) Quantification of PDCoV infection. Amount of cells and PDCoV$^+$ cells were counted using five or more pictures for each infection condition, and expressed relative to infection in mock-transfected HeLa cells.

Laval, QC, Canada (33); mouse anti-TGEV monoclonal antibody (ab20301) and mouse anti-HA epitope tag antibody (ab130275) were purchased from Abcam. The mouse monoclonal anti- PDCoV NP antigen antibody was purchased from Medgene Labs. Mouse monoclonal anti-dsRNA (J2) was purchased from Scicons. ST, African green monkey kidney (Vero-CCL81) cells, Madin-Darby canine kidney (MDCK) cells, human Huh7, DF-1, LLC-PK1, human embryonic kidney 293 cells stably expressing the SV40 large T antigen (HEK-293T), and derivatives of these cell lines were maintained in DMEM (Lonza BE12-741F) supplemented with 10% FBS (Bodinco). ST and Huh7 APN knockout cells have been described previously (44). LMH cells were maintained on plates coated with 0.1% gelatin in Waymouth's media supplemented with 10% nonheat-inactivated FBS and 1× penicillin/streptomycin. Cell lines stably expressing pAPN (GenBank accession no. NP_999442.1) were made using the Moloney murine leukemia virus (MoMLV) transduction system (Clontech) by means of a pQCXIN retroviral vector encoding a pAPN cDNA sequence C-terminally extended with an HA-tag (YPYDVPDYA). Stably transfected pAPN cells were selected and maintained with G418 (PAA Laboratories).

Reference strain PDCoV virus was purchased from the US Department of Agriculture and was propagated and titrated on LLC-PK1 cells in DMEM with 1 μg/mL TPCK-treated trypsin (4370285, Sigma). PDCoV strain FD22 (passage 101) (23), which was propagated and titrated on ST cells, was used in infection experiments analyzed by flow cytometry. TGEV strain Purdue (GenBank accession no. ABG89335.1) was propagated and titrated on PD5 porcine kidney cells. HCoV-229E was also propagated and titrated in DMEM supplemented with 1% of FBS but on human Huh7 cells.

Plasmid Design and Protein Expression. pCAGGS mammalian expression vectors encoding PDCoV S1 (isolate USA/Minnesota454/2014, residues 1–524; GB: AML40825.1) and its domain B (S1^B, residues 298–425) C-terminally extended with the Fc domain of human or mouse IgG were generated as described before (44). Similarly, expression plasmids were made encoding Fc-tagged S1 subunits of TGEV (isolate Purdue, GenBank accession no. ABG89335.1, residues 1–785), HCoV-229E (GenBank accession no. NP_073551.1, residues 1–537), as well as constructs encoding human Fc-tagged soluble APN ectodomains (i.e., nonmembrane anchored) of swine (pAPN, GenBank accession no. XP_005653580.1), chicken (gAPN, GenBank accession no. ACZ95799.1; kindly provided by M. H. Verheije, Utrecht University, Utrecht, The Netherlands), human (hAPN, GenBank accession no. NP_001141.2), and cat (fAPN, NP_001009252.2) (44). Plasmids encoding the APN–hFc fusion proteins were polyethylenimine (PEI)-transfected into 60% confluent HEK-293T cells for 6 h, after which transfections were removed and medium was replaced with 293 SFM II-based expression medium (Gibco Life Technologies) and incubated at 37 °C in 5% CO_2. Tissue culture supernatants were harvested 5–6 d posttransfection, and expressed proteins were purified using Protein A Sepharose beads (GE Healthcare) according to the manufacturer's instruction. Purity and integrity of all purified recombinant proteins was checked by SDS/PAGE. Purified proteins were stored at 4 °C until further use.

Immunofluorescence Assay. For immunofluorescence staining, cells were washed twice with PBS and fixed with 3.7% formaldehyde (Merck, 1040031000) in PBS, followed by membrane permeabilization with 0.1% Triton X-100 (Sigma, 93426) in PBS for 10 min at room temperature. Fixed cells were blocked using 3% BSA (GE Healthcare Life Sciences) in PBS for 1 h followed by incubation with the primary antibody for 1 h in PBS with 1% BSA. Cells were washed three times and staining was completed by Alexa Fluor 488-conjugated goat α-rabbit antibody (A11008, Life Technologies) or Alexa Fluor 488-conjugated goat α-mouse antibody (A11001, Life Technologies). Nuclei were visualized using DAPI nuclear counterstaining (D-9542, Sigma). Pictures of immunofluorescent cells were captured using an EVOS FL Cell Imaging System (ThermoFisher Scientific) at 10× magnification or a Leica SPE-II confocal microscope (40× magnification). Relative infection was calculated by counting and averaging the percentage of infected cells in at least five microscopic fields per condition.

APN-Based Solid-Phase Binding Assay. The ability of the CoV S1- and $S1^B$-mFc fusion proteins to bind hFc-tagged soluble APN ectodomains was evaluated by means of an APN-based solid-phase binding assay. Per well, 100 μL of soluble APN-hFc (10 μg/mL, diluted in PBS) was coated in a 96-well MaxiSorp plates (Nunc) by overnight incubation at 4 °C. Nonspecific binding sites were subsequently blocked with a 3% (wt/vol) solution of BSA in PBS. Plates were washed with PBS with 0.05% Tween-20 and subsequently incubated with serially diluted S1- or $S1^B$-mFc proteins (equimolar concentrations were used to assess relative binding affinities) for 1 h at room temperature, after which plates were washed three times with PBS with 0.05% Tween-20. Murine Fc-tagged S1 proteins were detected with horse radish peroxidase (HRP)-conjugated polyclonal rabbit α-mouse immunoglobulins (1:2,000 dilution in PBS with 1% BSA; DAKO, P0260), and a colorimetric reaction was initiated through incubation with 100 μL/well TMB (tetramethylbenzidine) Super Slow One Component HRP Microwell Substrate (GenWay Biotech, GWB-7CCD49) and stopped through addition of 12.5% H_2SO_4 (Merck). Optical density (OD) was subsequently measured at 450 nm with an ELISA reader (EL-808, BioTek). Background signal (α-mFc HRP-conjugate alone) was subtracted from the $OD_{450\ nm}$ values. TGEV and HCoV-229E S1-mFc fusion proteins were used as binding controls.

PDCoV Infection Experiments. The cell culture conditions used to infect different cells with PDCoV were as follows: washing of cells with PBS two times, virus incubation for 2 h in fresh DMEM containing 0.5 μg/mL (in ST, Huh7, HeLa-R19, LMH, DF-1 cells and their derivatives) or in fresh DMEM containing 1 μg/mL (in Vero cells and its derivatives) of TPCK-treated trypsin (Sigma, 4370285). Cells were fixed and permeabilized at 12 h postinfection (hpi) and stained with virus-specific antisera.

Syncytium Formation Assay. Parental and mutant ST cells were inoculated with PDCoV at a MOI = 0.01 in DMEM containing 0.5 μg/mL trypsin at 37 °C. After 2 h, the inoculum was replaced by maintenance medium (without trypsin) and cells were further incubated at 37 °C to permit viral replication and consequent S protein cell surface accumulation. After 16 h, medium was replaced with DMEM or DMEM supplemented with 0.5 μg/mL trypsin for 3 h to induce proteolytic activation of exposed PDCoV S proteins and consequent cell–cell fusion, and subjected to immunostaining.

Flow Cytometric Quantification of CoV Infection. Cells that had been plated 1 d prior were switched to enhanced MEM media (Gibco) containing 1% antibiotic-antimyotic (Gibco), 1% Hepes (Gibco), 1% (vol/vol) pancreatin (Sigma), and inoculated at a MOI = 1.0 for 1 h at 37 °C, after which inoculate was replaced by primary growth media containing 1% (vol/vol) pancreatin and cells were incubated overnight at 37 °C. Cells were fixed overnight in 100% EtOH at 4 °C, subsequently blocked for 1 h using 1× Power Bock Universal Blocking Reagent (Biogenex) at room temperature and stained overnight at 4 °C using a PDCoV-specific monoclonal antibody directed against the N protein (1:500; SDSU, mAb 55–197). TGEV staining was performed using a mix of two mAbs directed against the TGEV N protein (1:500; 25H7 and 14E3), which had been characterized previously (72–74). Cells were washed twice in PBS-T (PBS containing 0.1% Tween-20) before secondary antibody (1:400; goat α-mouse IgG Alexa488; Invitrogen) staining for 1 h at 37 °C. Cells were washed twice in PBS-T, resuspended in PBS, and analyzed using an Accuri C6 flow cytometer (BD Biosciences). A minimum of 20,000 events from three independent experiments was analyzed.

Flow Cytometric Analysis of Spike–Receptor Interactions. Human HeLa-R19 cells (ATCC) that had been plated 1 d prior were mock-transfected or transfected with APN encoding plasmids using FuGene 6. Twenty-four hours after transfection, cells were released from tissue-culture dishes using 1 mM EDTA solution, washed, fixed in formaldehyde solution (4%), and blocked for 30 min on ice in PBS supplemented with 10% goat serum. Cells were subsequently surface-stained with a rabbit anti-HA IgG antibody (1:1,600; Immune Systems, RHGT-45A-Z) and CoV $S1^{(B)}$-mFc proteins and corresponding secondary antibodies [goat α-rabbit IgG Alexa488 (1:200; Life Technologies); donkey α-mouse IgG Cy5 (1:200; Jackson Laboratory)] for 45 min in FACS buffer (PBS supplemented with 2% FCS, 5 mM EDTA and 0.02% NaN_3) on ice to analyze expression levels and CoV S receptor engagement, respectively. Cells were washed twice after both primary and secondary staining and ultimately resuspended in FACS buffer supplemented with 4% formaldehyde before analysis on BD FACSCanto (BD Biosciences) with Cyflogic software.

ACKNOWLEDGMENTS. We thank Raoul J. de Groot for critical reading of the manuscript and Leah Everitt for technical assistance. We thank the Center for Cell Imaging of the Utrecht Faculty of Veterinary Medicine for advice and assistance. This study is supported by TOP Project Grant (40-00812-98-13066) funded by ZonMW (to F.J.M.v.K. and B.-J.B.).

1. Geoghegan JL, Duchêne S, Holmes EC (2017) Comparative analysis estimates the relative frequencies of co-divergence and cross-species transmission within viral families. *PLoS Pathog* 13:e1006215.
2. Kitchen A, Shackelton LA, Holmes EC (2011) Family level phylogenies reveal modes of macroevolution in RNA viruses. *Proc Natl Acad Sci USA* 108:238–243.
3. World Health Organization (2015) Summary of probable SARS cases with onset of illness from 1 November 2002 to 31 July 2003. Available at www.who.int/csr/sars/country/table2004_04_21/en/. Accessed January 29, 2018.
4. Li W, et al. (2005) Receptor and viral determinants of SARS-coronavirus adaptation to human ACE2. *EMBO J* 24:1634–1643.
5. de Wit E, van Doremalen N, Falzarano D, Munster VJ (2016) SARS and MERS: Recent insights into emerging coronaviruses. *Nat Rev Microbiol* 14:523–534.
6. Graham RL, Baric RS (2010) Recombination, reservoirs, and the modular spike: Mechanisms of coronavirus cross-species transmission. *J Virol* 84:3134–3146.
7. Vijgen L, et al. (2006) Evolutionary history of the closely related group 2 coronaviruses: Porcine hemagglutinating encephalomyelitis virus, bovine coronavirus, and human coronavirus OC43. *J Virol* 80:7270–7274.
8. Corman VM, et al. (2016) Link of a ubiquitous human coronavirus to dromedary camels. *Proc Natl Acad Sci USA* 113:9864–9869.
9. Corman VM, et al. (2015) Evidence for an ancestral association of human coronavirus 229E with bats. *J Virol* 89:11858–11870.
10. Tao Y, et al. (2017) Surveillance of bat coronaviruses in Kenya identifies relatives of human coronaviruses NL63 and 229E and their recombination history. *J Virol* 91:1–16.
11. Lau SKP, et al. (2015) Discovery of a novel coronavirus, China *Rattus* coronavirus HKU24, from Norway rats supports the murine origin of Betacoronavirus 1 and has implications for the ancestor of Betacoronavirus lineage A. *J Virol* 89:3076–3092.
12. Hulswit RJ, de Haan CA, Bosch BJ (2016) Coronavirus spike protein and tropism changes. *Adv Virus Res* 96:29–57.
13. Woo PCY, et al. (2012) Discovery of seven novel mammalian and avian coronaviruses in the genus deltacoronavirus supports bat coronaviruses as the gene source of alphacoronavirus and betacoronavirus and avian coronaviruses as the gene source of gammacoronavirus and deltacoronavirus. *J Virol* 86:3995–4008.
14. Le VP, et al. (2017) A novel strain of porcine deltacoronavirus in Vietnam. *Arch Virol* 163:203–207.
15. Li G, et al. (2014) Full-length genome sequence of porcine deltacoronavirus strain USA/IA/2014/8734. *Genome Announc* 2:e00278–e14.
16. Marthaler D, Jiang Y, Collins J, Rossow K (2014) Complete genome sequence of strain SDCV/USA/Illinois121/2014, a porcine deltacoronavirus from the United States. *Genome Announc* 2:e00218–e14.
17. Wang L, Byrum B, Zhang Y (2014) Detection and genetic characterization of deltacoronavirus in pigs, Ohio, USA, 2014. *Emerg Infect Dis* 20:1227–1230.
18. Janetanakit T, et al. (2016) Porcine deltacoronavirus, Thailand, 2015. *Emerg Infect Dis* 22:757–759.
19. Lorsirigool A, et al. (2016) The first detection and full-length genome sequence of porcine deltacoronavirus isolated in Lao PDR. *Arch Virol* 161:2909–2911.
20. Song D, et al. (2015) Newly emerged porcine deltacoronavirus associated with diarrhoea in swine in China: Identification, prevalence and full-length genome sequence analysis. *Transbound Emerg Dis* 62:575–580.
21. Mai K, et al. (2018) The detection and phylogenetic analysis of porcine deltacoronavirus from Guangdong Province in Southern China. *Transbound Emerg Dis* 65:166–173.
22. Lee S, Lee C (2014) Complete genome characterization of Korean porcine deltacoronavirus strain KOR/KNU14-04/2014. *Genome Announc* 2:4–5.
23. Hu H, et al. (2015) Isolation and characterization of porcine deltacoronavirus from pigs with diarrhea in the United States. *J Clin Microbiol* 53:1537–1548.
24. Dong N, et al. (2015) Porcine deltacoronavirus in mainland China. *Emerg Infect Dis* 21:2254–2255.

25. Ma Y, et al. (2015) Origin, evolution, and virulence of porcine deltacoronaviruses in the United States. *MBio* 6:e00064.
26. Jung K, et al. (2015) Pathogenicity of 2 porcine deltacoronavirus strains in gnotobiotic pigs. *Emerg Infect Dis* 21:650–654.
27. de Groot RJ, Baker S, Baric RS, Ziebuhr J (2011) Coronaviridae. *Virus Taxonomy: Ninth Report of the International Committee on Taxonomy of Viruses*, eds King AMQ, Adams MJ, Carstens EB, Lefkowitz EJ (Elsevier, London), pp 806–828.
28. Walls AC, et al. (2016) Cryo-electron microscopy structure of a coronavirus spike glycoprotein trimer. *Nature* 531:114–117.
29. Walls AC, et al. (2016) Glycan shield and epitope masking of a coronavirus spike protein observed by cryo-electron microscopy. *Nat Struct Mol Biol* 23:899–905.
30. Kirchdoerfer RN, et al. (2016) Pre-fusion structure of a human coronavirus spike protein. *Nature* 531:118–121.
31. Xiong X, et al. (2017) Glycan shield and fusion activation of a deltacoronavirus spike glycoprotein fine-tuned for enteric infections. *J Virol* 92:1–16.
32. Shang J, et al. (2017) Cryo-EM structure of porcine delta coronavirus spike protein in the pre-fusion state. *J Virol* 92:1–14.
33. Williams RK, Jiang GS, Holmes KV (1991) Receptor for mouse hepatitis virus is a member of the carcinoembryonic antigen family of glycoproteins. *Proc Natl Acad Sci USA* 88:5533–5536.
34. Yeager CL, et al. (1992) Human aminopeptidase N is a receptor for human coronavirus 229E. *Nature* 357:420–422.
35. Delmas B, et al. (1992) Aminopeptidase N is a major receptor for the enteropathogenic coronavirus TGEV. *Nature* 357:417–420.
36. Raj VS, et al. (2013) Dipeptidyl peptidase 4 is a functional receptor for the emerging human coronavirus-EMC. *Nature* 495:251–254.
37. Hofmann H, et al. (2005) Human coronavirus NL63 employs the severe acute respiratory syndrome coronavirus receptor for cellular entry. *Proc Natl Acad Sci USA* 102:7988–7993.
38. Li W, et al. (2003) Angiotensin-converting enzyme 2 is a functional receptor for the SARS coronavirus. *Nature* 426:450–454.
39. Li W, et al. (2017) Identification of sialic acid-binding function for the Middle East respiratory syndrome coronavirus spike glycoprotein. *Proc Natl Acad Sci USA* 114: E8508–E8517.
40. Matrosovich M, Herrler G, Klenk HD (2015) Sialic acid receptors of viruses. *Top Curr Chem* 367:1–28.
41. Winter C, Schwegmann-Wessels C, Cavanagh D, Neumann U, Herrler G (2006) Sialic acid is a receptor determinant for infection of cells by avian infectious bronchitis virus. *J Gen Virol* 87:1209–1216.
42. Huang X, et al. (2015) Human coronavirus HKU1 spike protein uses O-acetylated sialic acid as an attachment receptor determinant and employs hemagglutinin-esterase protein as a receptor-destroying enzyme. *J Virol* 89:7202–7213.
43. Kolb AF, Maile J, Heister A, Siddell SG (1996) Characterization of functional domains in the human coronavirus HCV 229E receptor. *J Gen Virol* 77:2515–2521.
44. Li W, et al. (2017) Aminopeptidase N is not required for porcine epidemic diarrhea virus cell entry. *Virus Res* 235:6–13.
45. Bausch-Fluck D, et al. (2015) A mass spectrometric-derived cell surface protein atlas. *PLoS One* 10:e0121314.
46. Li BX, Ge JW, Li YJ (2007) Porcine aminopeptidase N is a functional receptor for the PEDV coronavirus. *Virology* 365:166–172.
47. Shirato K, Matsuyama S, Ujike M, Taguchi F (2011) Role of proteases in the release of porcine epidemic diarrhea virus from infected cells. *J Virol* 85:7872–7880.
48. Chen L, Lin Y-L, Peng G, Li F (2012) Structural basis for multifunctional roles of mammalian aminopeptidase N. *Proc Natl Acad Sci USA* 109:17966–17971.
49. Delmas B, et al. (1994) Determinants essential for the transmissible gastroenteritis virus-receptor interaction reside within a domain of aminopeptidase-N that is distinct from the enzymatic site. *J Virol* 68:5216–5224.
50. Tresnan DB, Levis R, Holmes KV (1996) Feline aminopeptidase N serves as a receptor for feline, canine, porcine, and human coronaviruses in serogroup I. *J Virol* 70: 8669–8674.
51. Mina-Osorio P (2008) The moonlighting enzyme CD13: Old and new functions to target. *Trends Mol Med* 14:361–371.
52. Dijkman R, et al. (2013) Isolation and characterization of current human coronavirus strains in primary human epithelial cell cultures reveal differences in target cell tropism. *J Virol* 87:6081–6090.
53. van der Velden VHJ, et al. (1998) Expression of aminopeptidase N and dipeptidyl peptidase IV in the healthy and asthmatic bronchus. *Clin Exp Allergy* 28:110–120.
54. Kenny AJ, Maroux S (1982) Topology of microvillar membrance hydrolases of kidney and intestine. *Physiol Rev* 62:91–128.
55. Jung K, Hu H, Saif LJ (2016) Porcine deltacoronavirus infection: Etiology, cell culture for virus isolation and propagation, molecular epidemiology and pathogenesis. *Virus Res* 226:50–59.
56. Millet JK, Whittaker GR (2015) Host cell proteases: Critical determinants of coronavirus tropism and pathogenesis. *Virus Res* 202:120–134.
57. Tusell SM, Schittone SA, Holmes KV (2007) Mutational analysis of aminopeptidase N, a receptor for several group 1 coronaviruses, identifies key determinants of viral host range. *J Virol* 81:1261–1273.
58. Kolb AF, Hegyi A, Siddell SG (1997) Identification of residues critical for the human coronavirus 229E receptor function of human aminopeptidase N. *J Gen Virol* 78: 2795–2802.
59. Wu K, Li W, Peng G, Li F (2009) Crystal structure of NL63 respiratory coronavirus receptor-binding domain complexed with its human receptor. *Proc Natl Acad Sci USA* 106:19970–19974.
60. Earnest JT, et al. (2017) The tetraspanin CD9 facilitates MERS-coronavirus entry by scaffolding host cell receptors and proteases. *PLoS Pathog* 13:e1006546.
61. Drexler JF, Corman VM, Drosten C (2014) Ecology, evolution and classification of bat coronaviruses in the aftermath of SARS. *Antiviral Res* 101:45–56.
62. Vijaykrishna D, et al. (2007) Evolutionary insights into the ecology of coronaviruses. *J Virol* 81:4012–4020.
63. Menachery VD, Graham RL, Baric RS (2017) Jumping species-a mechanism for coronavirus persistence and survival. *Curr Opin Virol* 23:1–7.
64. Barlan A, et al. (2014) Receptor variation and susceptibility to Middle East respiratory syndrome coronavirus infection. *J Virol* 88:4953–4961.
65. Raj VS, et al. (2014) Adenosine deaminase acts as a natural antagonist for dipeptidyl peptidase 4-mediated entry of the Middle East respiratory syndrome coronavirus. *J Virol* 88:1834–1838.
66. Woolhouse M, Scott F, Hudson Z, Howey R, Chase-Topping M (2012) Human viruses: Discovery and emergence. *Philos Trans R Soc Lond B Biol Sci* 367:2864–2871.
67. Jung K, Hu H, Saif LJ (2017) Calves are susceptible to infection with the newly emerged porcine deltacoronavirus, but not with the swine enteric alphacoronavirus, porcine epidemic diarrhea virus. *Arch Virol* 162:2357–2362.
68. Dong BQ, et al. (2007) Detection of a novel and highly divergent coronavirus from Asian leopard cats and Chinese ferret badgers in Southern China. *J Virol* 81: 6920–6926.
69. Robinson TP, et al. (2011) *Global Livestock Production Systems* (FAO, Rome).
70. Shi Y, Wu Y, Zhang W, Qi J, Gao GF (2014) Enabling the 'host jump': Structural determinants of receptor-binding specificity in influenza A viruses. *Nat Rev Microbiol* 12: 822–831.
71. Weatherman S, Feldmann H, de Wit E (2018) Transmission of henipaviruses. *Curr Opin Virol* 28:7–11.
72. Welch SK, Saif LJ (1988) Monoclonal antibodies to a virulent strain of transmissible gastroenteritis virus: Comparison of reactivity with virulent and attenuated virus. *Arch Virol* 101:221–235.
73. Simkins RA, Weilnau PA, Bias J, Saif LJ (1992) Antigenic variation among transmissible gastroenteritis virus (TGEV) and porcine respiratory coronavirus strains detected with monoclonal antibodies to the S protein of TGEV. *Am J Vet Res* 53:1253–1258.
74. Lin C-M, et al. (2015) Antigenic relationships among porcine epidemic diarrhea virus and transmissible gastroenteritis virus strains. *J Virol* 89:3332–3342.
75. Santiago C, et al. (2017) Allosteric inhibition of aminopeptidase N functions related to tumor growth and virus infection. *Sci Rep* 7:46045.